THE ASTROPHYSICAL JOURNAL, 549:402–415, 2001 March 1

TRANSPORT PHENOMENA IN STOCHASTIC MAGNETIC MIRRORS

LEONID MALYSHKIN AND RUSSELL KULSRUD
Princeton University Observatory, Princeton, NJ 08544; leonmal@astro.princeton.edu, rkulsrud@astro.princeton.edu
Received 2000 August 21; accepted 2000 October 18

ABSTRACT

Parallel thermal conduction along stochastic magnetic field lines may be reduced because the heat-conducting electrons become trapped and detrapped between regions of strong magnetic field (magnetic mirrors). The problem reduces to a simple but realistic model for diffusion of monoenergetic electrons based on the fact that when there is a reduction of diffusion, it is controlled by a subset of the mirrors, the principal mirrors. The diffusion reduction can be considered as equivalent to an enhancement of the pitch angle scattering rate. Therefore, in deriving the collision integral, we modify the pitch angle scattering term. We take into account the full perturbed electron-electron collision integral, as well as the electron-proton collision term. Finally, we obtain the four plasma transport coefficients and the effective thermal conductivity. We express them as reductions from the classical values. We present these reductions as functions of the ratio of the magnetic field decorrelation length to the electron mean free path at the thermal speed $V_T = (2kT/m_e)^{1/2}$. We briefly discuss an application of our results to clusters of galaxies.

Subject headings: conduction — diffusion — magnetic fields — methods: analytical — plasmas

1. INTRODUCTION

The problem of thermal conduction in a stochastic magnetic field is crucial for our understanding of galaxy cluster formation (Suginohara & Ostriker 1998; Cen & Ostriker 1999) and for the theory of cooling flows (Fabian 1990). It is also of great interest for solar physics and for various questions of plasma physics. At the same time, the question of whether or not electron thermal conduction is so strongly inhibited by a stochastic magnetic field in a galaxy cluster that it can be neglected is a very controversial one (Rosner & Tucker 1989; Tribble 1989; Tao 1995; Pistinner & Shaviv 1996; Chandran & Cowley 1998). It is currently estimated that if the coefficient of thermal conductivity is less than 1/30 of the Spitzer value, then the timescale of the heat conduction in the cluster is more than the Hubble time (Suginohara & Ostriker 1998). Otherwise, thermal conduction is important.[1]

The problem of thermal diffusion of heat-conducting electrons in a stochastic magnetic field should be divided into two separate parts because there are two separate effects that reduce diffusion in the presence of a stochastic magnetic field (Pistinner & Shaviv 1996; Chandran, Cowley, & Ivanushkina 1999). The first effect is that the heat-conducting electrons have to travel along tangled magnetic field lines, and as a result, they have to go larger distances between hot and cold regions of space. (In other words, the temperature gradients are weaker along magnetic field lines.) The second effect is that electrons, while they are traveling along the field lines, become trapped and detrapped between magnetic mirrors (which are regions of strong magnetic field). A trapped electron is reflected back and forth between magnetic mirrors until collisions make its pitch angle sufficiently small for the electron to escape the magnetic trap.

In this paper we concentrate on the second effect, and we derive the reduction of the effective electron thermal conduction parallel to the magnetic field lines caused by the presence of stochastic magnetic mirrors.

As is well known, a temperature gradient produces electrical current as well as heat flow. Similarly, an electric field produces heat flow as well as current. The four transport coefficients describing this are given in equations (34) and (35). The transport coefficients were first calculated by Spitzer & Härm for an unmagnetized plasma (Cohen, Spitzer, & Routly 1950; Spitzer & Härm 1953). Their coefficients also apply in an uniform magnetic field for transport parallel to the field. In this paper, we show how the parallel transport coefficients can be reduced in the presence of stochastic magnetic mirrors, and we calculate their reduced values by the same kinetic approach as that of Spitzer & Härm. The reduction factors are presented in Figure 5. The reduced effective thermal conductivity (that resulting when the electric field is present to cancel the current) is given in Figure 6. Spatial diffusivity of monoenergetic electrons along the magnetic field lines is presented in Figure 3.

First, in § 2, we solve the kinetic equation to find the escape time τ_m for electrons trapped between two equal magnetic mirrors. We assume that all electrons have a single value of speed, V, i.e., they are monoenergetic. The exact calculations of the escape time are given in Appendices A and B. In addition, we carry out Monte Carlo particle simulations to confirm our results.

Second, in § 3, we apply our results for this escape time to find the reduction of diffusion of monoenergetic electrons in a system of stochastic mirrors. It turns out that in the limit $l_0 \gg \lambda$, where l_0 is the magnetic field decorrelation length and λ is the electron mean free path, the parallel diffusivity is unaffected by magnetic mirrors and is given by the standard value $D_0 = (1/3)V\lambda$. In the opposite limit, $l_0 \ll \lambda$, magnetic mirrors do reduce diffusivity. We find that in this case there is a subset of the mirrors, the principal mirrors, that inhibits diffusion the most. These are mirrors whose separation distances are approximately equal to the electron *effective mean free path*, $\lambda_{\rm eff}$, the typical distance that electrons travel in the loss cones before they are scattered out of them. In order to estimate the reduction of diffusion in this limit, we need consider only the principal mirrors, neglecting all

[1] This numerical estimate, 1/30 of the Spitzer value, is based on numerical simulations with limited resolution, so it is not the last word on the problem.

others. Again, we perform the numerical simulations to support these theoretical results.

Third, in § 4, in order to carry out a precise kinetic treatment involving all electrons, we consider the diffusion reduction to be equivalent to an enhancement of the pitch angle scattering rate of electrons. In deriving the collision integral, we, therefore, modify the pitch angle scattering term by the inverse of the factor by which the spatial diffusion is reduced. We take into account the full perturbed electron-electron collision integral, as well as the electron-proton collision term. We obtain an integrodifferential equation for the perturbed electron distribution function in the presence of stochastic magnetic mirrors. If there is no reduction of electron diffusivity, our equation reduces to the well-known result obtained by Spitzer & Härm (Cohen et al. 1950; Spitzer & Härm 1953; Spitzer 1962).

Fourth, in § 5, we solve our equation numerically, separately for the Lorentz gas in the presence of magnetic mirrors, neglecting electron-electron collisions (in this case the equation simplifies greatly), and for the Spitzer gas in the presence of magnetic mirrors. We find the reductions of the four plasma transport coefficients and of the effective thermal conductivity as functions of the ratio of the magnetic field decorrelation length l_0 to the electron mean free path at the thermal speed $V_T = (2kT/m_e)^{1/2}$ (this mean free path is different for the Lorentz and Spitzer models). We find that the major effect of the magnetic mirrors is the reduction of anisotropy of superthermal electrons (this anisotropy is driven by a temperature gradient or/and by an electric field). Electrical current and heat are mainly transported by these electrons, whose diffusivity is suppressed the most.

Finally, we discuss our results and give the conclusions in § 6.

2. MONOENERGETIC ELECTRONS TRAPPED BETWEEN TWO EQUAL MAGNETIC MIRRORS

In this section we solve the kinetic equation to find the escape time τ_m for electrons trapped between two equal magnetic mirrors. We assume here and in the next section that all electrons have a single value of speed, V, which is unchanged by collisions; i.e., electrons are monoenergetic. In order to derive an analytical solution, we make several additional simplifying assumptions. Let the two magnetic barriers (mirrors) both be equal to B_m, and we assume the magnetic field B is constant between them. We introduce the mirror strength $m \equiv B_m/B$. The separation of the mirrors is l_m, and their thicknesses are negligible compared to l_m. In other words, magnetic mirrors are similar to thin step functions with heights $B_m - B$ and with constant field B between them (see Fig. 1). This is a reasonable assumption, because as we will see in the next section, electron diffusion is controlled by strong mirrors with mirror strengths $m \gtrsim 4$, which are separated by distances much larger than the magnetic field decorrelation length (if the spectrum of mirrors falls off with their strength significantly faster than $1/m$, the case that we consider in this paper).

Under these assumptions, the kinetic equation for the distribution function $f(t, x, \mu)$ of monoenergetic electrons trapped between the two mirrors is (Braginskii 1965)

$$\frac{\partial f}{\partial t} + \mu V \frac{\partial f}{\partial x} = \frac{\nu}{2} \frac{\partial}{\partial \mu} \left[(1 - \mu^2) \frac{\partial f}{\partial \mu} \right]. \tag{1}$$

Here x is a one-dimensional space coordinate along a magnetic flux tube, t is time, $\mu = \cos\theta$ is the cosine of the electron's pitch angle, and $\nu = V/\lambda$ is the collision frequency (λ is the mean free path, see eqs. [43] and [46]). The right-hand side of equation (1) represents the pitch angle scattering rate, ν, of electrons. The electrons are trapped in the region of space between the mirrors, $-l_m/2 < x < l_m/2$, and they can escape through the two windows, $x = l_m/2$, $\mu > \mu_{\rm crit} = (1 - 1/m)^{1/2}$, and $x = -l_m/2$, $\mu < -\mu_{\rm crit}$, as shown in Figure 1. The mirror strength is $m = B_m/B$, and it is the measure of the relative heights of the magnetic barriers. For simplicity, we assume that the barriers are high, i.e., $m \gg 1$ and $\mu_{\rm crit} \approx 1 - 1/2m$. In this case the electron distribution is in quasi-static equilibrium,

$$f(t, x, \mu) = e^{-t/\tau_m} F(x, \mu), \quad \tau_m \gg \nu^{-1}, \tag{2}$$

and equation (1) reduces to

$$-\frac{F}{\tau_m} + \mu V \frac{\partial F}{\partial x} = \frac{\nu}{2} \frac{\partial}{\partial \mu} \left[(1 - \mu^2) \frac{\partial F}{\partial \mu} \right]. \tag{3}$$

Let us consider an electron traveling in the loss cone $\mu > \mu_{\rm crit} = (1 - 1/m)^{1/2} \approx 1 - 1/2m$ (or $\mu < -\mu_{\rm crit}$). The

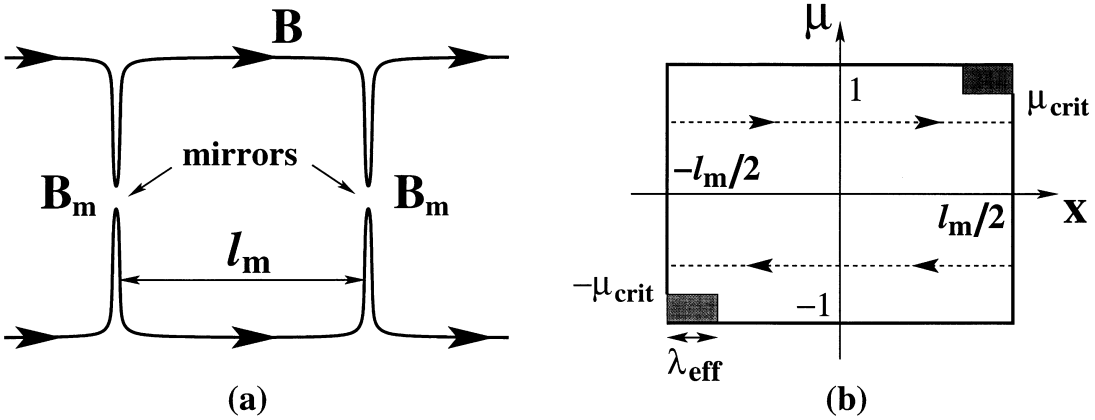

FIG. 1.—(*a*) Magnetic flux tube with two "step function–like" magnetic mirrors. The mirror strengths are $m = B_m/B$. (*b*) Phase space box where electrons are trapped in coordinates x and $\mu = \cos\theta$. The horizontal dotted lines show a closed trajectory of a trapped electron in the limit $l_m \ll \lambda$. The electrons escape the magnetic trap through two escape windows: $x = l_m/2$, $\mu > \mu_{\rm crit} = (1 - 1/m)^{1/2}$ and $x = -l_m/2$, $\mu < -\mu_{\rm crit}$. In the limit $l_m \ll \lambda_{\rm eff}$, the electrons freely escape to the right or left whenever they reach the two loss cones, $\mu > \mu_{\rm crit}$ and $\mu < -\mu_{\rm crit}$. In the opposite limit, $\lambda_{\rm eff} \ll l_m$, the electrons escape when they reach the two shaded regions of the phase space.

effective electron mean free path, which is the typical distance the electron travels before it is scattered by small-angle collisions out of the loss cone, is

$$\lambda_{\rm eff} \equiv \lambda/2m \ll \lambda \, . \tag{4}$$

In other words, $\lambda_{\rm eff}$ is a decay distance for a flow of electrons traveling in the loss cones. The solution of equation (3) and, therefore, the escape time τ_m depend on the mirror strength m and the ratio l_m/λ. There are three limiting cases for which simple approximate solutions exist: (1) $l_m \ll \lambda_{\rm eff} = \lambda/2m$, (2) $\lambda_{\rm eff} \ll l_m \ll \lambda^2/\lambda_{\rm eff} = 2m\lambda$, and (3) $\lambda^2/\lambda_{\rm eff} \ll l_m$. We solve equation (3) for case (1) in Appendix A and for cases (2) and (3) in Appendix B, and we obtain the electron escape times

$$\begin{aligned}
&\tau_m^{(1)} = \nu^{-1} \ln m, \quad l_m \ll \lambda_{\rm eff} \, , \\
&\tau_m^{(2)} = \nu^{-1}(l_m/\lambda_{\rm eff}) = \nu^{-1}(2ml_m/\lambda), \ \lambda_{\rm eff} \ll l_m \ll \lambda^2/\lambda_{\rm eff} \, , \\
&\tau_m^{(3)} = \nu^{-1}(3/\pi^2)(l_m/\lambda)^2, \ \lambda^2/\lambda_{\rm eff} \ll l_m \, .
\end{aligned} \tag{5}$$

The following simple physical arguments help to understand these results in these three limiting cases. The collisional scattering is a two-dimensional random walk of a unit vector (which is the direction of the electron velocity) on a surface of a unit-radius sphere with frequency ν [so the scattered angle $\Delta_s = (2\nu t)^{1/2}$ after time interval t]. The right-hand side of the kinetic equation (1) represents a one-dimensional random walk in μ-space that follows from the two-dimensional walk because of symmetry. However, it is convenient for the moment to return to the original two-dimensional scattering because it is isotropic. The angular sizes of the two loss cones on the unit-radius sphere are $\Delta_{\rm esc} \approx 1/\sqrt{m}$. First, in the limit $l_m \ll \lambda_{\rm eff}$, collisions are very weak, and the scattered angle over the travel time between mirrors, l_m/V, is $\sim (l_m/\lambda)^{1/2} \ll \Delta_{\rm esc}$. Therefore, in this case we can disregard the electron motion in x-space. We divide the surface of the unit-radius sphere into $\sim m$ boxes, each of angular size $\sim \Delta_{\rm esc} \approx 1/\sqrt{m}$. The time it takes for the unit vector to random walk from one box to another is $\sim \nu^{-1}/m$, resulting in the total escape time $\tau_m \sim m(\nu^{-1}/m) = \nu^{-1}$. Because the unit vector can "visit" each box more than once, the exact result contains the logarithm of m. Second, in the limit $\lambda_{\rm eff} \ll l_m \ll \lambda^2/\lambda_{\rm eff}$, we have to consider motion in x-space as well. In this case the electrons move in three-dimensional phase space, and they escape when they are in the two loss cones within distance $\lambda_{\rm eff}$ from the mirrors, as shown by the shaded regions in Figure 1*b*. We divide the three-dimensional phase space into $\sim (l_m/\lambda_{\rm eff})(1/\Delta_{\rm esc}^2) \sim m^2 l_m/\lambda$ boxes, each of size $\lambda_{\rm eff}\Delta_{\rm esc}^2 \sim \lambda/m$. The time it takes to move from one box to another is $\sim \nu^{-1}/m$, resulting in the total escape time $\tau_m \sim (m^2 l_m/\lambda)(\nu^{-1}/m) = \nu^{-1}(ml_m/\lambda)$. Note that the electron distribution function is almost constant in the phase space in this case (see Appendix B). Third, in the limit $\lambda^2/\lambda_{\rm eff} \ll l_m$, the escape of electrons is controlled by slow diffusion in x-space, so the escape time is approximately equal to the time of diffusion between mirrors, $\tau_m \sim \nu^{-1}(l_m/\lambda)^2$ in this case.

In our further calculations we use a simple interpolation formula

$$\tau_m \approx \tau_m^{(1)} + \tau_m^{(2)} + \tau_m^{(3)} = \nu^{-1}[\ln m + (l_m/\lambda_{\rm eff}) + (3/\pi^2)(l_m/\lambda)^2] \tag{6}$$

for the whole range of parameters m and l_m/λ. This formula is suggested by the numerical simulations shown in Figure 2. The dots in this figure show the results of our Monte Carlo particle simulations for three mirror strengths $m = 2$, $m = 16$, and $m = 128$. To obtain our simulation results we followed 10^3–10^6 electrons trapped between two equal magnetic mirrors separated by distance l_m ranging from 1/1024 to 256 in units of the mean free path λ. We carry out Monte Carlo simulations in the following way: First, initially all particles have $x = 0$ and $\mu = 0$. Second, the cosine of the pitch angle of each particle random walks inside interval $(-1, 1)$ according to equation (1); i.e., the change of μ in time interval $dt \ll 1/\nu$ is $d\mu = \pm\{[1 - (\mu + d\mu)^2]\nu\, dt\}^{1/2}$. Here + or − are chosen randomly with equal probabilities, and $d\mu$ is given implicitly (the implicit method guarantees that $-1 < \mu < 1$; the square root can be expanded in $\nu\, dt \ll 1$). The change of particle position x in time interval dt is obviously $dx = \mu V\, dt$. Third, each particle escapes the mirror trap whenever $\mu > \mu_{\rm crit}$ and $x = l_m/2$, or $\mu < -\mu_{\rm crit}$ and $x = -l_m/2$. Independently of the initial distribution of electrons, the number of trapped electrons tends to an exponential dependence on time with the characteristic decay time τ_m in just a few collision times (see eq. [2]). The solid lines in the figure represent formula (6) and are in a very good agreement with the simulations even for the smallest mirror strength $m = 2$.

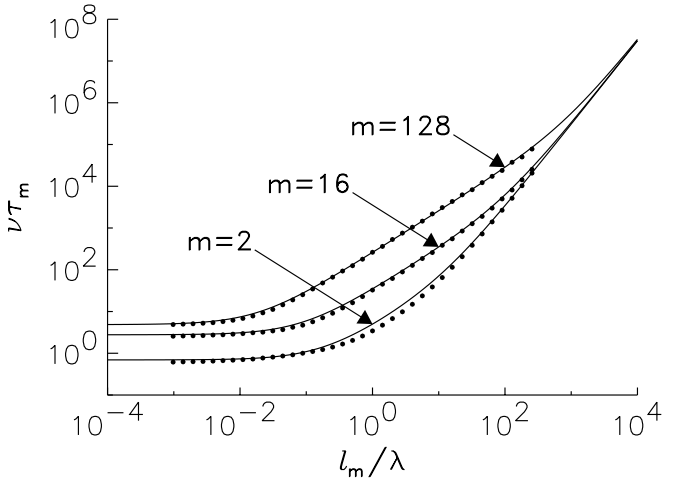

FIG. 2.—The dots show a logarithmic plot of the numerically obtained electron escape time τ_m in units of the collision time ν^{-1} as a function of the separation l_m of two equal magnetic mirrors in units of the mean free path λ. These results are based on our Monte Carlo particle simulations of 10^3–10^6 trapped electrons, assuming three values of the mirror strengths, $m = 2$, $m = 16$, and $m = 128$. The solid lines represent the analytical result (eq. [6]).

3. DIFFUSION OF MONOENERGETIC ELECTRONS IN A SYSTEM OF RANDOM MAGNETIC MIRRORS

In this section we continue to assume that electrons have a single value of speed, V. If there were no magnetic mirrors and the magnetic field had constant strength along the field lines, the parallel diffusion of monoenergetic electrons would be the standard spatial diffusion, $D_0 = (1/3)V\lambda$. Here λ is the electron mean free path at speed V. However, as we have discussed in the introductory section, diffusing electrons move along flux tubes with random magnetic field strength and become trapped and detrapped between magnetic mirrors. These mirrors are regions of strong field and are separated by a field decorrelation length l_0. As a result,

the diffusion is reduced by a factor that depends on the ratio l_0/λ.

In the main part of this section we derive this diffusion analytically and at the end of the section confirm it with numerical simulations. (In contrast to the previous section, where there were only two equal mirrors, in this section we consider many mirrors with random spacing and strength.)

Consider the limit $l_0 \gg \lambda$ first. In this case collisions are strong, and according to the third formula in equation (5), the time it takes for electrons to escape a trap between two magnetic mirrors is independent of the mirror strengths and is entirely controlled by the standard spatial diffusion transport of electrons between the mirrors. As a result, magnetic mirrors can be ignored, and there is no reduction of diffusion, $D = D_0$.

In the opposite limit, $l_0 \ll \lambda$, the collisions are weak, and magnetic mirrors do result in a reduction of diffusion. To find this reduction, we divide all mirrors into equal-size bins $b_m = (m - \delta/2,\ m + \delta/2]$, where m is the bin central mirror strength and constant δ is the width of the bins (the value of δ will be discussed later).

For the moment we consider the diffusion in the presence of only those mirrors that are in a single bin b_m. It turns out that one of the bins leads to a smaller diffusion than any other bin, and the net diffusion due to all the mirrors is approximately that due to only mirrors in this bin, provided that the bins are sufficiently wide.

Let the spectrum of magnetic mirror strengths be $\mathscr{P}(m)$. We assume that strong magnetic mirrors are rare; i.e., the spectrum falls off fast with the mirror strength (we will estimate how fast it should fall off, below). The probability that a mirror belongs to bin b_m is

$$p_m = \int_{m-\delta/2}^{m+\delta/2} \mathscr{P}(m')\, dm' \approx \delta \mathscr{P}(m) + (\delta^3/24)\mathscr{P}''(m)\ . \quad (7)$$

At each decorrelation length l_0, the magnetic field changes and becomes decorrelated. Therefore, the mean separation of mirrors that are in bin b_m is

$$l_m = l_0 \sum_{k=1}^{\infty} k p_m (1 - p_m)^{k-1} = l_0/p_m\ . \quad (8)$$

Let us consider an electron trapped between two mirrors of bin b_m. The time τ_m that it takes for this electron to escape the trap is given by equation (6), where we keep only the first two terms (because $l_0 \ll \lambda$)

$$\tau_m \approx \tau_m^{(1)} + \tau_m^{(2)} = v^{-1} \ln (m q_m)\ . \quad (9)$$

Here, we introduce the important parameter

$$q_m \equiv \exp\,(l_m/\lambda_{\rm eff}) = \exp\,(2ml_0/p_m\lambda)\ , \quad (10)$$

where the mean distance l_m between the two mirrors is given by equation (8). After the electron escapes, it travels freely in the loss cone in one of the two directions along the magnetic field lines until it is again trapped between another two mirrors of bin b_m. The freely traveling electron becomes first trapped with probabilities $1 - e^{-l_m/\lambda_{\rm eff}} = 1 - q_m^{-1}$ in $0 \le x < l_m$, $e^{-l_m/\lambda_{\rm eff}} - e^{-2l_m/\lambda_{\rm eff}} = q_m^{-1} - q_m^{-2}$ in $l_m \le x < 2l_m$, $e^{-2l_m/\lambda_{\rm eff}} - e^{-3l_m/\lambda_{\rm eff}} = q_m^{-2} - q_m^{-3}$ in $2l_m \le x < 3l_m$, and so on. Therefore, the mean distance squared $\langle \Delta x^2 \rangle_m$ that the electron travels in the loss cones before trapping is

$$\langle \Delta x^2 \rangle_m \approx l_m^2 \sum_{k=1}^{\infty} k^2 (q_m^{-k+1} - q_m^{-k}) = l_m^2 \frac{q_m(q_m+1)}{(q_m-1)^2}\ . \quad (11)$$

The processes of trapping and detrapping repeat in time intervals τ_m. In other words, electrons random walk along the field lines in a system of mirrors that belong to bin b_m with steps $\approx \langle \Delta x^2 \rangle_m$ in time intervals $\approx \tau_m$. As a result, the diffusion coefficient for these electrons is $D(m) = C(\langle \Delta x^2 \rangle_m / 2\tau_m)$, where we introduce a scaling constant C, which is of the order unity and will be determined by the numerical simulations. The corresponding reduction of diffusion is

$$D(m)/D_0 = C\,\frac{3}{2}\left(\frac{l_0}{\lambda}\right)^2 \frac{q_m(q_m+1)}{(q_m-1)^2}\,\frac{1}{p_m^2}\,\frac{1}{\ln(mq_m)}\ , \quad l_0 \ll \lambda\ , \quad (12)$$

where we use $D_0 = (1/3)v\lambda^2$ and equations (8), (9), and (11), and p_m and q_m are given by equations (7) and (10).

For a given spectrum of mirrors $\mathscr{P}(m)$ and given constants δ and C, the diffusion reduction (12) due to mirrors of bin b_m is a function of mirror strength m. Let us analyze this function in two limits: $\ln q_m \ll 1$ and $\ln q_m \gg \ln m \gtrsim 1$. If $\ln q_m \ll 1$, then $q_m - 1 = 2ml_0/p_m\lambda \ll 1$. Therefore, $D(m)/D_0 \approx C(3/4)(1/m^2 \ln m)$ and $(d/dm)[D(m)/D_0] < 0$. On the other hand, if $\ln q_m \gg \ln m$, then $D(m)/D_0 \approx C(3/4)(l_0/\lambda)(1/mp_m)$. Therefore, $(d/dm)[D(m)/D_0] > 0$ if the spectrum of mirrors falls off faster than $1/m$ with the mirror strength.[2] In this paper we make an assumption that the spectrum falls off significantly faster than $1/m$.

Therefore, a minimum of $D(m)/D_0$ exists. Let this minimum be achieved at $m = m_p$. Then $\ln q_{m_p} = l_{m_p}/\lambda_{\rm eff} \sim 2/\ln m_p \sim 1$, or $l_{m_p} \sim \lambda_{\rm eff}$. The minimum can roughly be estimated as $D(m_p)/D_0 = \min\,[D(m)/D_0] \sim 1/m_p^2$, which is in agreement with the qualitative results of Albright et al. (2000).

In other words, if $l_0 \ll \lambda$, then there is the bin that inhibits diffusion the most. We call it the principal bin, $b_p = (m_p - \delta/2,\ m_p + \delta/2]$. The corresponding mirror strength m_p is the principal mirror strength. The minimum of diffusion $D(m)$ due to mirrors of bin b_m is achieved at the principal strength, $m = m_p$. The spacing of the mirrors that are in the principal bin is of the order of the effective mean free path for this bin, $l_{m_p} \sim \lambda_{\rm eff} = \lambda/2m_p$. The main idea is that, in order to estimate the net diffusion due to all mirrors, we need consider only magnetic mirrors that are in the principal bin and we can neglect all other bins. Mirrors that are smaller than the principal mirrors "work" poorly in the inhibition of diffusion because they are weak and are separated by distances less than $\lambda_{\rm eff}$ (which is the distance that electrons travel in the loss cones). Mirrors that are larger than the principal mirrors "work" poorly, because they are very rare and are separated by very large distances (provided the mirror spectrum falls off with the mirror strength significantly faster than $1/m$). Of course, occasionally there will be a larger mirror between two principal mirrors, since they have to be somewhere, but if the distribution falls off rapidly with the mirror strength (see eq. [14]), this occurs only very rarely and, as confirmed by our numerical simulations, does not affect the statistical results.

[2] This criterion is different from the result of Albright et al. (2000), who found $1/m^2$ to be the boundary spectrum for the transition between their diffusive and subdiffusion regimes. We believe that the difference arises because, for flat spectra, our bin width δ starts to depend on l_0/λ (and our simple diffusion model breaks down).

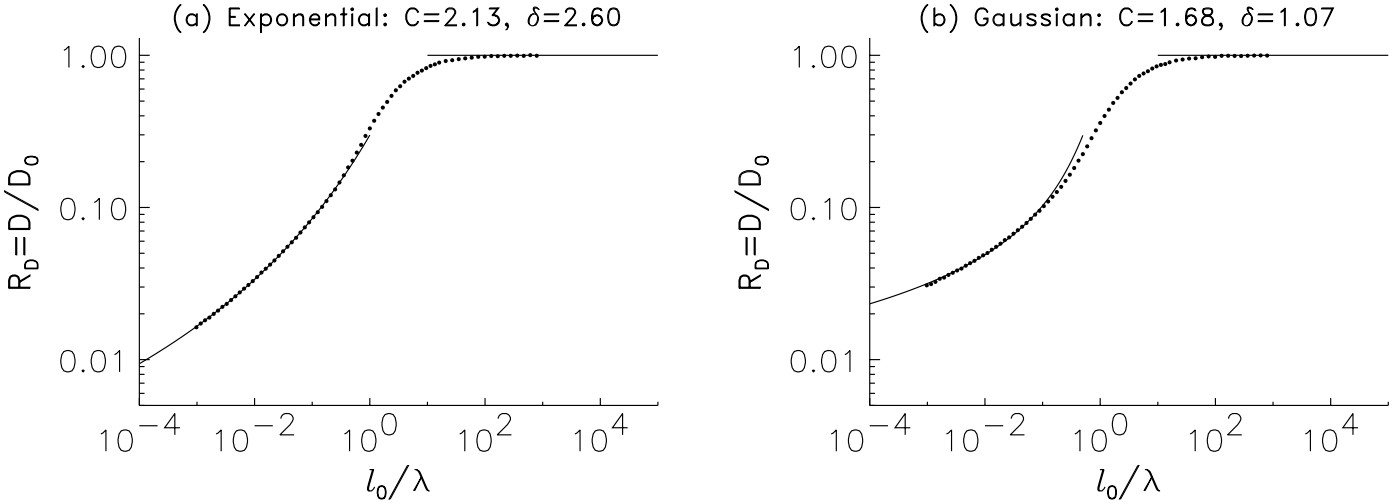

FIG. 3.—We consider two mirror spectra: (*a*) exponential and (*b*) Gaussian (see eq. [14]). The dots show the reduction of diffusion, $R_D = D/D_0$, obtained by Monte Carlo particle simulations of (1–6) × 10^5 electrons, each followed in a system of magnetic mirrors over 300 collision times ν^{-1}. The solid lines represent the theoretical results given by eq. (13). The constants C and δ are obtained by matching the theoretical results with the results of simulations for each of the two spectra (and these constants do not depend on l_0/λ).

The theoretical results based on these assumptions fit nicely our simulation results for large and small λ/l_0 (see Fig. 3).

As a result of these considerations, we can combine our theoretical results for the reduction of diffusion of monoenergetic electrons, $R_D = D/D_0$, into a single formula valid in the two limits for l_0/λ,

$$R_D = D/D_0 = \begin{cases} \min\limits_m [D(m)/D_0] = D(m_p)/D_0 , & l_0 \ll \lambda , \\ 1 , & l_0 \gg \lambda , \end{cases} \tag{13}$$

where $D(m)/D_0$ is given by equation (12) and the minimum is achieved at the principal mirror strength $m = m_p$ (note that $\ln q_{m_p} = l_{m_p}/\lambda_{\rm eff} \sim 1$).

We show the theoretical monoenergetic diffusion reduction (13) by the solid lines in Figure 3 for two mirror spectra: exponential and Gaussian,[3]

$$\mathcal{P}(m) = \begin{cases} e^{-(m-2)} & \text{exponential} , \\ (2/\pi)^{1/2} e^{-(m-2)^2/2} & \text{Gaussian} . \end{cases} \tag{14}$$

The results of our Monte Carlo particle simulations are shown by dots. The constants C and δ (*top*) are of the order unity, and we adjust them by matching our theoretical results with the results of simulations in the case of each of the two spectra (C and δ do not depend on l_0/λ). The simulations are based on (1–6) × 10^5 particles. For each particle we choose a distribution of mirrors $m \geq 2$. These are placed at $x = 0, \pm l_0, \pm 2l_0, \pm 3l_0, \ldots$; i.e., all mirrors are separated by the magnetic field decorrelation length l_0. The strengths of all mirrors are chosen (for each particle) according to the assumed mirror spectrum (14). Initially, all particles start in the middle between two mirrors, $x = l_0/2$, and particles have zero cosine of the pitch angle, $\mu = 0$. We evolve μ and x of each particle in the way that was described in the previous section, except now when particles reach the loss cones, they are allowed to move from one mirror trap to another. We follow the particles during 300 collision times ν^{-1} after their distribution relax in couple collision times. Then we average the particle displacements squared $\langle \Delta x^2 \rangle$ at a given time t to obtain the diffusion coefficient $\langle \Delta x^2 \rangle / 2t$ given in Figure 3.

Note that the bin width δ is larger for the exponential spectrum than it is for the Gaussian. This is because the latter is steeper at large mirror strengths. Figures 4*a* and 4*b* clearly demonstrate the difference. In these figures we plot the natural logarithm of the diffusion reduction (12) caused by mirrors that are in bin b_m versus the mirror strength m for $l_0/\lambda = 1/16$ and for both spectra (eq. [14]) of mirror strengths. The principal bins are shown by arrows. In the case of each spectrum, the reduction has the minimum at the corresponding principal mirror strength m_p. We see that the reduction roughly doubles over its minimal value at the boundaries of the principal bin, $m = m_p + \delta/2$ and $m = m_p - \delta/2$.

4. THE FOKKER-PLANCK KINETIC EQUATION

In this section we use the results found above to obtain a modified kinetic equation to describe electrons traveling in a system of random magnetic mirrors. The reduction of spatial diffusion of monoenergetic electrons with speed V, R_D, was obtained in the previous section. However, mirrors reduce only the electron spatial diffusion, and they hardly affect the diffusion and flux of the averaged probability distribution of electrons in velocity (energy) space. Therefore, in order to represent the spatial diffusion reduction in the familiar form of the Fokker-Planck equation, we note that such a reduction would be achieved by a distribution of electrons with an enhanced pitch angle scattering rate, since the pitch angle scattering is directly related to spatial diffusion. (Of course, for any case in which the diffusion is reduced significantly, our description really refers to a time average of the kinetic equation over a time interval long compared to a bounce time between mirrors, during which the pitch angle of any particle changes finitely.) We believe that the two electron distributions, one with an enhanced pitch angle scattering and no mirrors, and the other our distribution in mirrors with no enhanced scattering, behave the same way as far as transport phenomena are considered.

[3] We find the minimum in eq. (13) numerically.

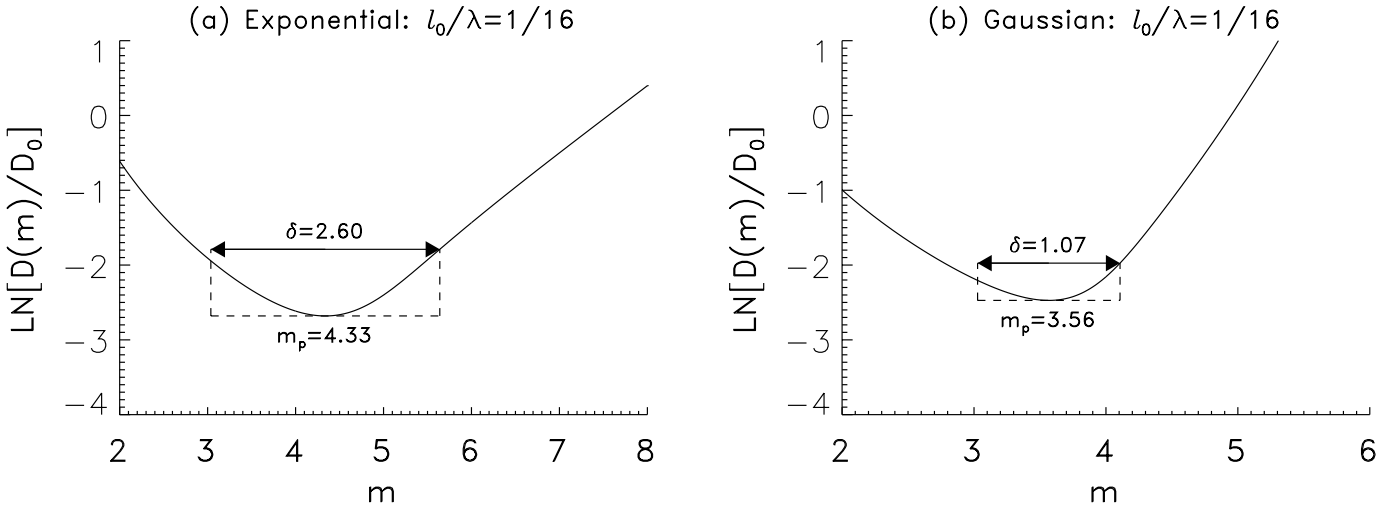

FIG. 4.—Natural logarithm of the diffusion reduction (12) caused by mirrors that are in bin b_m for $l_0/\lambda = 1/16$. We consider two mirror spectra: (*a*) exponential and (*b*) Gaussian (see eq. [14]). The principal bins are shown by arrows. In the case of each spectrum, the reduction has the minimum at the principal mirror strength m_p, and it roughly doubles at the boundaries of the principal bin.

As a result, hereafter we consider only the first electron distribution, and in deriving the collision integral, we modify the pitch angle scattering term by factor R_D^{-1}, where R_D is the factor by which the spatial diffusion is reduced (see the previous section). R_D does depend on electron speed, so we no longer assume electrons to be monoenergetic. We take into account the full perturbed electron-electron collision integral, as well as the electron-proton collision term. When $R_D \equiv 1$, our equations reduce to those of Spitzer & Härm (Cohen et al. 1950; Spitzer & Härm 1953; Spitzer 1962).

The electron distribution function is

$$f(\mu, V) = f_0(V) + f_1(\mu, V) , \tag{15}$$

where f_0 is the zero-order isotropic part given by the Maxwellian distribution,

$$f_0 = n(x)[m_e/2\pi kT(x)]^{3/2} e^{-m_e V^2/2kT(x)} = n\pi^{-3/2} V_T^{-3} e^{-v^2} , \tag{16}$$

and $f_1 \propto \mu$ is the first-order anisotropic perturbation (of order the temperature gradient and electric field)

$$f_1(\mu, V) = \mu n V_T^{-3} S(v) . \tag{17}$$

Here m_e is the electron mass, k is the Boltzmann constant, and the electron temperature $T(x)$ and concentration $n(x)$ slowly change in space. We also introduce the dimensionless electron speed $v = V/V_T$, where the thermal electron speed is $V_T = (2kT/m_e)^{1/2}$. Thus, the function $S(v)$ in equation (17) is dimensionless.

In a steady state, the kinetic equation for the electrons is obviously

$$V_x(\partial f_0/\partial x) - (eE/m_e)(\partial f_0/\partial V_x) = (\delta f/\delta t)_c , \tag{18}$$

where $(\delta f/\delta t)_c$ is the Coulomb collision integral that includes electron-proton and electron-electron collisions, $V_x = \mu V$ is the x-component of the electron velocity (the component along the magnetic field lines), and E is the electric field in the x-direction. The electron pressure should be constant, $P = kn(x)T(x) = \text{const}$.[4] As a result, the derivatives of the Maxwellian electron distribution are

$$\partial f_0/\partial x = (v^2 - 2.5)(f_0/T)(dT/dx) ,$$
$$\partial f_0/\partial V_x = -(2\mu/V_T) v f_0 . \tag{19}$$

The collision integral is divided up as

$$(\delta f/\delta t)_c = (\delta f_0/\delta t)_0 + (\delta f_1/\delta t)_0 + (\delta f_0/\delta t)_1$$
$$= (\delta f_1/\delta t)_0 + (\delta f_0/\delta t)_1 , \tag{20}$$

where $(\delta f_0/\delta t)_0 \equiv 0$ corresponds to Maxwellian collisions acting on f_0, $(\delta f_1/\delta t)_0$ corresponds to Maxwellian collisions (with enhanced pitch angle scattering) acting on f_1, and $(\delta f_0/\delta t)_1$ corresponds to perturbed collisions acting on f_0 (since f_0 is isotropic, there is no pitch angle scattering in this collision term). The collision integral (20) can be best obtained, in the Fokker-Planck form, by using the Rosenbluth potentials $h(\mu, V) = h_0(V) + h_1(\mu, V)$ and $g(\mu, V) = g_0(V) + g_1(\mu, V)$ (Rosenbluth, MacDonald, & Judd 1957). Here h_0 and g_0 are calculated using the Maxwellian parts of the electron and ion distribution functions in equation (16), while the perturbed potentials, $h_1 = 2\mu\mathscr{A}_1(V)$ and $g_1 = \mu\mathscr{B}_1(V)$, are proportional to μ, and they are calculated using the perturbed part of the electron distribution function (17).

The Maxwellian potentials h_0 and g_0 determine the $(\delta f_1/\delta t)_0$ part of the Fokker-Planck collision integral, and the perturbed potentials, $h_1 = 2\mu\mathscr{A}_1(V)$ and $g_1 = \mu\mathscr{B}_1(V)$, are used to find the $(\delta f_0/\delta t)_1$ part of the Fokker-Planck collision integral (see eq. [31] of Rosenbluth et al. 1957),

$$(\delta f_1/\delta t)_0 = \frac{A_D}{2n}\left\{-\frac{1}{V^2}\frac{\partial}{\partial V}\left(f_1 V^2 \frac{dh_0}{dV}\right) + \frac{1}{2V^2}\frac{\partial^2}{\partial V^2}\right.$$
$$\times\left(f_1 V^2 \frac{d^2 g_0}{dV^2}\right) - \frac{1}{V^2}\frac{\partial}{\partial V}\left(f_1 \frac{dg_0}{dV}\right)$$
$$\left. + R_D^{-1}\frac{1}{2V^3}\frac{dg_0}{dV}\frac{\partial}{\partial \mu}\left[(1-\mu^2)\frac{\partial f_1}{\partial \mu}\right]\right\} , \tag{21}$$

[4] Because the hydrodynamic timescale is much shorter than the transport, e.g., thermal conduction, timescale.

$$(\delta f_0/\delta t)_1 = \mu \frac{A_D}{2n}\left[-\frac{2}{V^2}\frac{d}{dV}\left(f_0 V^2 \frac{d\mathscr{A}_1}{dV}\right) + \frac{4}{V^2} f_0 \mathscr{A}_1 + \frac{1}{2V^2}\frac{d^2}{dV^2}\left(f_0 V^2 \frac{d^2\mathscr{B}_1}{dV^2}\right) - \frac{3}{V^3} f_0 \frac{d\mathscr{B}_1}{dV} + \frac{3}{V^4} f_0 \mathscr{B}_1 - \frac{3}{V^2}\frac{d}{dV} \times \left(f_0 \frac{d\mathscr{B}_1}{dV}\right) + \frac{3}{V^2}\frac{d}{dV}\left(f_0 \frac{\mathscr{B}_1}{V}\right)\right]. \quad (22)$$

For a hydrogen plasma the "diffusion constant" A_D is

$$A_D = 8\pi n e^4 \ln\Lambda / m_e^2 , \quad (23)$$

where e is the absolute value of the electron charge and $\ln\Lambda$ is the Coulomb logarithm (Spitzer 1962). Note that the last term in equation (21) is the pitch angle scattering term, and we multiply it by our enhancement factor R_D^{-1} (compare this term with the right-hand side of eq. [1]).

Using equations (17) and (18) of Rosenbluth et al. (1957), we express the derivatives of the potentials h_0 and g_0 in terms of the three Maxwellian diffusion coefficients $\langle \Delta V_\parallel \rangle_0$, $\langle (\Delta V_\perp)^2 \rangle_0$, and $\langle (\Delta V_\parallel)^2 \rangle_0$, which are further given in terms of error functions (see eqs. [5-15]–[5-20] of Spitzer 1962)

$$dh_0/dV = (2n/A_D)\langle \Delta V_\parallel \rangle_0 = -(n/V^2)[1 + 4v^2 G(v)] ,$$
$$dg_0/dV = (n/A_D)V\langle (\Delta V_\perp)^2 \rangle_0 = n[1 + \Phi(v) - G(v)] ,$$
$$d^2 g_0/dV^2 = (2n/A_D)\langle (\Delta V_\parallel)^2 \rangle_0 = (2n/V)G(v) . \quad (24)$$

Here Φ is the usual error function, and G is expressed in terms of Φ and its derivative Φ'; they are functions of the dimensionless speed $v = V/V_T$ [$V_T = (2kT/m_e)^{1/2}$],

$$\Phi(v) = (2/\sqrt{\pi})\int_0^v e^{-x^2} dx, \quad G(v) = \frac{\Phi(v) - v\Phi'(v)}{2v^2} . \quad (25)$$

The perturbed potentials, $h_1 = 2\mu\mathscr{A}_1(V)$ and $g_1 = \mu\mathscr{B}_1(V)$, are calculated using the perturbed electron distribution function (17) and are given by the following formulae (see eqs. [40], [41], [45], and [46] of Rosenbluth et al. 1957):

$$\mathscr{A}_1 = (4\pi/3)(n/V_T)[v^{-2}\bar{I}_3(S; v) + v\underline{I}_0(S; v)] ,$$
$$\mathscr{B}_1 = (4\pi/3)nV_T[0.2v^{-2}\bar{I}_5(S; v) - \bar{I}_3(S; v) - v\underline{I}_2(S; v) + 0.2v^3\underline{I}_0(S; v)] , \quad (26)$$

where we introduce integrals

$$\bar{I}_m(S; v) = \int_0^v v^m S(v)\, dv, \quad \underline{I}_m(S; v) = \int_v^\infty v^m S(v)\, dv . \quad (27)$$

Now, substituting equations (16), (17), (24), and (26) into formulae (21) and (22), and using definitions (25) and (27) and equation (20), after considerable algebra, we have for the collision integrals

$$(\delta f_1/\delta t)_0 = (nA_D/2V_T^6)\mu v^{-2}(\hat{\mathscr{L}}S - 2v^2\Phi' S) ,$$
$$(\delta f_0/\delta t)_1 = (nA_D/2V_T^6)\mu v^{-2}(\hat{\mathscr{I}}S + 2v^2\Phi' S) ,$$
$$(\delta f/\delta t)_c = (nA_D/2V_T^6)\mu v^{-2}(\hat{\mathscr{L}}S + \hat{\mathscr{I}}S) , \quad (28)$$

where the differential and the integral operators are defined as

$$\hat{\mathscr{L}}S(v) = d/dv[vG(dS/dv)] + 2v^2 G(dS/dv) - [v^{-1}R_D^{-1}(1 + \Phi - G) - 4v^2\Phi']S , \quad (29)$$
$$\hat{\mathscr{I}}S(v) = (4/15\sqrt{\pi})e^{-v^2}[12\bar{I}_5(S; v) - 10\bar{I}_3(S; v) + 2v^3(6v^2 - 5)\underline{I}_0(S; v)] . \quad (30)$$

The enhancement of the Maxwellian pitch angle scattering rate, R_D^{-1}, enters into the differential operator (29). The term R_D depends on the dimensionless speed $v = V/V_T$; we will explicitly give this dependence in equations (42) and (45).

Finally, substituting formulae (28) and (19) into equation (18), we obtain the kinetic equation for the dimensionless perturbed electron distribution function $S(v)$ (see eq. [17]),

$$\hat{\mathscr{L}}S = \gamma_T v^3(2v^2 - 5)e^{-v^2} + \gamma_E v^3 e^{-v^2} - \hat{\mathscr{I}}S , \quad (31)$$

$$S(v) \to 0, \quad \text{as } v \to 0 \text{ and as } v \to \infty , \quad (32)$$

where constants γ_T and γ_E are

$$\gamma_T = \frac{k^2 T}{2\pi^{5/2} n e^4 \ln\Lambda}\frac{dT}{dx} , \quad \gamma_E = \frac{kT}{\pi^{5/2} n e^3 \ln\Lambda} E . \quad (33)$$

We also take the obvious boundary conditions in equation (32) for function S. Equations (29)–(31) reduce to the Spitzer equations for an ionized hydrogen gas (Cohen et al. 1950; Spitzer & Härm 1953) if we set $R_D \equiv 1$ and make a substitution $S(v) = \pi^{-3/2}e^{-v^2}D(v)$. However, we prefer to use function S, because of the simpler boundary conditions in equation (32).

5. THE REDUCTION OF TRANSPORT COEFFICIENTS BY STOCHASTIC MAGNETIC MIRRORS

In a steady state, an electric field E and a temperature gradient dT/dx both produce anisotropic perturbations of the electron distribution function, $f_1(\mu, v) = \mu n V_T^{-3} S(v)$ (see eqs. [15] and [17]). This anisotropy results in an electron flow and, consequently, in an electric current j and in a heat flow Q along magnetic field lines (in the x-direction),

$$j = -e\int_0^\infty \int_{-1}^1 \mu V f_1\, d\mu 2\pi V^2\, dV = \sigma E + \alpha(dT/dx) , \quad (34)$$

$$Q = \int_0^\infty \int_{-1}^1 \mu V(m_e V^2/2) f_1\, d\mu 2\pi V^2\, dV = -\beta E - \kappa(dT/dx) . \quad (35)$$

Here σ, α, β, and κ are the four transport coefficients to be found (σ and κ are the electrical and thermal conductivities).

Before we proceed to the calculation of the transport coefficients, let us first call attention to the electron flow produced by the electric field. The electric field produces two different kinds of electron flow. The first, the main flow, is due to acceleration of electrons, which is described by the term containing E in equation (18) and correspondingly by the term containing γ_E in equation (31). The second, an additional flow, arises because the electric field changes the size of the two loss cones of a mirror trap, so in Figure 1*b* $\mu_{\rm crit}$ in the right upper corner is not equal to $\mu_{\rm crit}$ in the left lower corner. As a result, the electrons are more likely to escape the trap in the direction opposite to the electric field. Fortunately, this additional flow, which is rather complicated to find precisely, can be neglected compared to the flow due to acceleration. We give a proof of this in Appendix C.[5]

[5] The main reason is that the difference in the two loss cones due to electric field is inversely proportional to the electron kinetic energy, so the additional flow has a factor $1/V^2$ compared to a factor $1/V_T^2$ that enters the main flow due to acceleration. Because both the current and the heat flow are mainly transported by superthermal electrons $v = V/V_T \sim 2$, the additional flow is approximately 20% of the main flow (see Appendix C).

In further calculations, it is convenient to break $S(v)$ into the two separate inhomogeneous solutions of equation (31), which we denote as $S_T(v)$ and $S_E(v)$.[6] The first solution, S_T, is obtained by setting $\gamma_T = 1$ and $\gamma_E = 0$, and the second solution, S_E, is obtained by setting $\gamma_T = 0$ and $\gamma_E = 1$, i.e.,

$$S_T(v) = S(v), \quad \text{when } \gamma_T = 1 \text{ and } \gamma_E = 0 ,$$
$$S_E(v) = S(v), \quad \text{when } \gamma_T = 0 \text{ and } \gamma_E = 1 . \tag{36}$$

The general solutions to equation (31) and the perturbed distribution function (17) are the linear combinations of the two inhomogeneous solutions,

$$S(v) = \gamma_T S_T(v) + \gamma_E S_E(v) ,$$
$$f_1(\mu, v) = \mu n V_T^{-3}[\gamma_T S_T(v) + \gamma_E S_E(v)] . \tag{37}$$

In other words, S_T and S_E correspond to anisotropic perturbations of the electron distribution function, which are driven by the temperature gradient and by the electric field, respectively, while $S = \gamma_T S_T + \gamma_E S_E$ is the total anisotropic perturbation.

We now consider separately two cases: first, the Lorentz gas in a system of random mirrors, and second, the Spitzer gas in a system of random mirrors. For the Lorentz gas, electrons are assumed to collide only with protons, so equations (29)–(31) become greatly simplified. For the Spitzer gas, we consider both the electron-electron and the electron-proton collisions, so we solve the full set of our equations.

5.1. *Lorentz Gas in a System of Random Mirrors*

Here we assume that the electrons collide only with protons, so we have for operators (29) and (30)

$$\hat{\mathscr{L}} S = -S/v R_D, \quad \hat{\mathscr{I}} S = 0 , \tag{38}$$

resulting in the two simple inhomogeneous solutions in equation (36) of equation (31),

$$S_T(v) = -v^4(2v^2 - 5)e^{-v^2} R_D, \quad S_E(v) = -v^4 e^{-v^2} R_D . \tag{39}$$

If there are no magnetic mirrors, so $R_D \equiv 1$, we substitute equations (39) into formula (37) and easily carry out the two integrals in equations (34) and (35). Taking into consideration the definitions in equation (33), we obtain the well-known Lorentz transport coefficients (Spitzer 1962)

$$\sigma_L = 2\left(\frac{2}{\pi}\right)^{3/2} \frac{(kT)^{3/2}}{m_e^{1/2} e^2 \ln\Lambda} , \quad \alpha_L = 3\left(\frac{2}{\pi}\right)^{3/2} \frac{k(kT)^{3/2}}{m_e^{1/2} e^3 \ln\Lambda} ,$$
$$\beta_L = 8\left(\frac{2}{\pi}\right)^{3/2} \frac{(kT)^{5/2}}{m_e^{1/2} e^3 \ln\Lambda} , \quad \kappa_L = 20\left(\frac{2}{\pi}\right)^{3/2} \frac{k(kT)^{5/2}}{m_e^{1/2} e^4 \ln\Lambda} . \tag{40}$$

If there are magnetic mirrors, it is convenient to normalize the resulting transport coefficients to the corresponding Lorentz coefficients in equation (40). Substituting equation (37) into the two integrals in equations (34) and (35), and again using the definitions in equation (33), we have

$$\sigma/\sigma_L = -(1/3)\bar{I}_3(S_E; \infty), \quad \alpha/\alpha_L = -(1/9)\bar{I}_3(S_T; \infty) ,$$
$$\beta/\beta_L = -(1/12)\bar{I}_5(S_E;\infty), \quad \kappa/\kappa_L = -(1/60)\bar{I}_5(S_T;\infty) , \tag{41}$$

where the integral moments are defined by equation (27), and S_T and S_E are given by equation (39).

In order to find explicitly the diffusion reduction factor R_D in equation (39) as a function of v, we refer to the results of § 3. In that section we found the diffusion reduction as a function of the ratio of the magnetic field decorrelation length l_0 to the electron mean free path λ. For Lorentz electrons the mean free path λ_L is proportional to the fourth power of the electron speed, $\lambda_L \propto V^4$ (Spitzer 1962; Braginskii 1965). Thus, we have

$$R_D = R_D(l_0/\lambda_L) = R_D(v^{-4} l_0/\lambda_{L,T}) , \tag{42}$$

where $\lambda_{L,T}$ is obviously the Lorentz electron mean free path at the thermal speed $V_T = (2kT/m_e)^{1/2}$,

$$\lambda_{L,T} = (kT)^2/\pi n e^4 \ln\Lambda \approx 0.1 \text{ kpc}(T/10^7 \text{ K})^2(10^{-3} \text{ cm}^{-3}/n) . \tag{43}$$

Here we assume the Coulomb logarithm for a cluster of galaxies to be $\ln\Lambda \approx 40$ (Suginohara & Ostriker 1998).

We use our analytical results of equation (13) for the monoenergetic diffusion reduction $R_D = R_D(l_0/\lambda_L) = R_D(v^{-4} l_0/\lambda_{L,T})$ when $v^{-4} l_0/\lambda_{L,T} < 1/300$ and $v^{-4} l_0/\lambda_{L,T} > 300$ (the numerical simulations are extremely time consuming for very small and very large l_0/λ), and we use our numerical simulation results presented in Figure 3 for $v^{-4} l_0/\lambda_{L,T}$ in between. (We carry out the cubic spline interpolation of the simulation results. Note that R_D is not differentiated in operator [29], so our final results are not sensitive to small noise errors in the calculation of R_D.)

Using equations (39) and (42) with R_D given in § 3 and numerically performing the velocity integrals, we find all four transport coefficients in equation (41) normalized to the standard Lorentz coefficients in equation (40). The dashed lines in Figures 5*a*–5*h* show the resulting normalized transport coefficients σ, α, β, and κ as functions of $l_0/\lambda_{L,T}$ for the two mirror spectra: (*a*) exponential and (*b*) Gaussian (see eq. [14]). The asymptotic values of the coefficients at large values of $l_0/\lambda_{L,T}$ are given by the numbers on the dashed lines, and they are unity. Thus, there are no reductions of the transport coefficients at $l_0/\lambda_{L,T} \gg 1$, as one can expect because there is no reduction of electron diffusivity in this limit (see eq. [13]). In a steady state, the electrical current j in a highly ionized plasma should be zero. Thus, if a temperature gradient is present, the resulting electric field E is obtained by setting j to zero in equation (34). Substituting this result for E into equation for the heat flow (35), we find for the effective thermal conductivity

$$\kappa_{\text{eff}} = \kappa - \alpha\beta/\sigma ,$$
$$\kappa_{\text{eff}}/\kappa_L = \kappa/\kappa_L - (3/5)(\alpha/\alpha_L)(\beta/\beta_L)(\sigma_L/\sigma) , \tag{44}$$

where we use the formulae in equation (40) for the Lorentz transport coefficients in the second line of this equation.

Using the transport coefficients reported in Figure 5 by dashed lines and formula (44), it is easy to find the effective thermal conductivity κ_{eff} normalized to the standard Lorentz thermal conductivity κ_L (see eq. [40]). However, it is more useful to give the ratio of κ_{eff} to the Lorentz effective conductivity, $\kappa_{L,\text{eff}} = 0.4\kappa_L$. This ratio is the actual suppression of the effective conductivity of the Lorentz gas by magnetic mirrors. The dashed lines in Figure 6 show this suppression, $\kappa_{\text{eff}}/\kappa_{L,\text{eff}}$, as functions of $l_0/\lambda_{L,T}$ for the two mirror spectra: (*a*) exponential and (*b*) Gaussian (see eq. [14]). It has been estimated that the time of heat conduction in clusters of galaxies is possibly larger than the Hubble time if the thermal conductivity is less than 1/30 of the Spitzer value (Suginohara & Ostriker 1998). The horizontal dotted lines indicate this reduction of 1/30.

[6] The two homogeneous solutions of eq. (31) must be excluded, because they diverge either at $v \to 0$ or at $v \to \infty$, violating the conditions in eq. (32) (see more details in Cohen et al. [1950]).

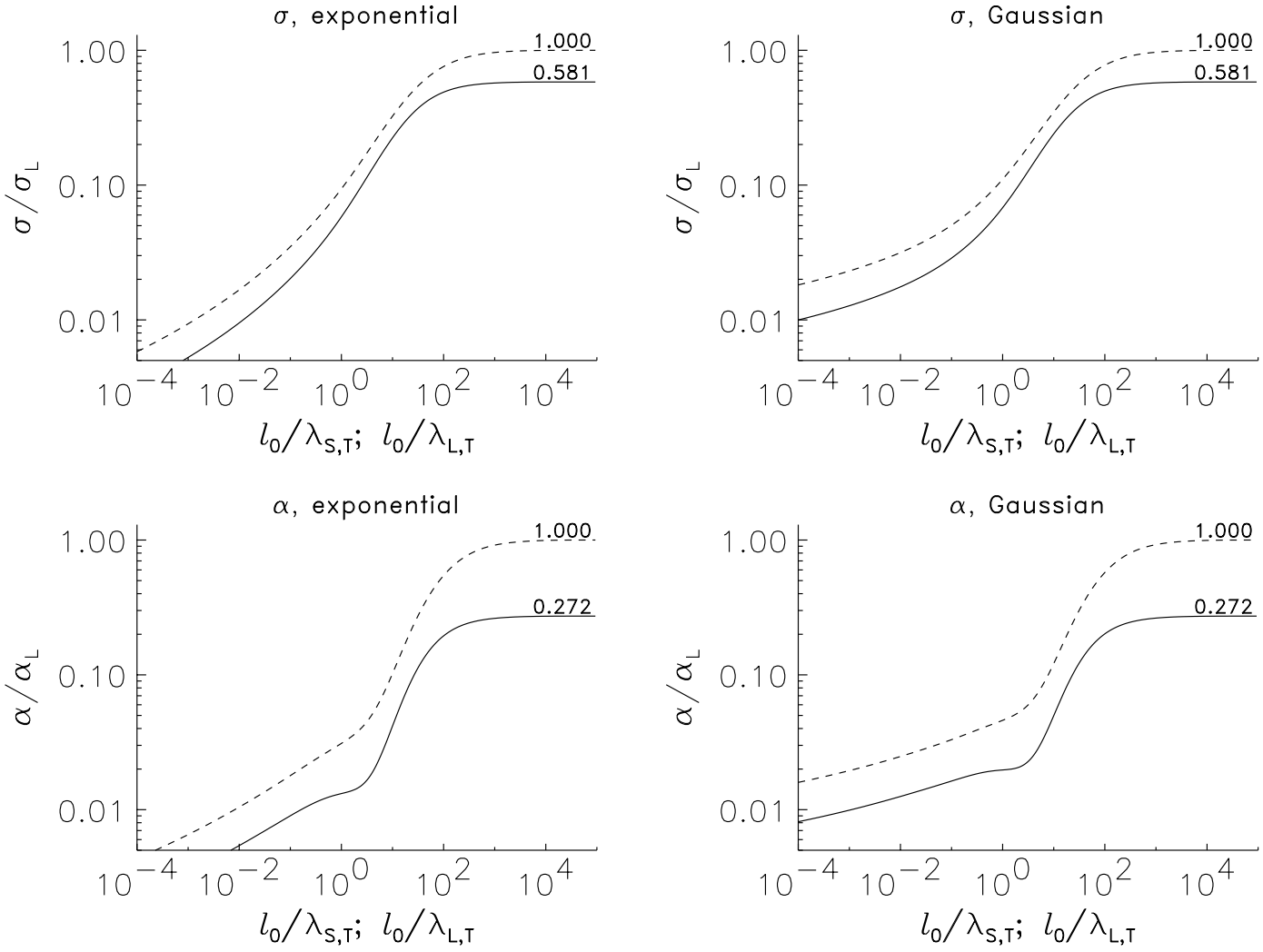

FIG. 5.—Panels on the left/right correspond to the exponential/Gaussian mirror spectra (see eq. [14]). The solid/dashed lines in all panels show the four transport coefficients, σ, α, β, and κ, for the Spitzer/Lorentz gas in the presence of stochastic magnetic mirrors as functions of the ratio of the magnetic field decorrelation length l_0 to the Spitzer/Lorentz electron mean free path, $\lambda_{S,T}/\lambda_{L,T}$, calculated at the electron thermal speed $V_T = (2kT/m_e)^{1/2}$ (see eqs. [43] and [46]). All transport coefficients are normalized to the standard Lorentz transport coefficients given by eq. (40). The asymptotic values of the coefficients at $l_0/\lambda_T \gg 1$ are given by the numbers on the lines. They agree with the results of Spitzer & Härm (1953).

For comparison, the dotted lines represent the monoenergetic diffusion reduction at the electron thermal speed, $R_D(l_0/\lambda_{L,T}) = D(l_0/\lambda_{L,T})/D_0$. We see that the Lorentz gas effective conductivity is reduced to a value 2–3 times smaller than that of the diffusion reduction. This is because heat is mainly transported by superthermal electrons. These electrons have long mean free paths, and the magnetic mirrors more strongly inhibit their diffusion.

5.2. *Spitzer Gas in a System of Random Mirrors*

Now consider the full collision integral (28) for the Spitzer gas in a system of random magnetic mirrors. We have numerically solved the full set of our equations (29)–(32). Formulae (41) and (44) remain the same as for the Lorentz gas, but the functions $S_T(v)$ and $S_E(v)$ are different. For Spitzer electrons the mean free path is $\lambda_S \propto V^4[1 + \Phi(v) - G(v)]^{-1}$ (Spitzer 1962; the error functions Φ and G are given by eq. [25]). Thus, formula (42) for the reduction of spatial diffusivity now becomes

$$R_D = R_D(l_0/\lambda_S) = R_D\left(v^{-4}\,\frac{l_0}{\lambda_{S,T}}\,\frac{1+\Phi(v)-G(v)}{1+\Phi(1)-G(1)}\right), \quad (45)$$

where the Spitzer electron mean free at the thermal speed $V_T = (2kT/m_e)^{1/2}$ is

$$\lambda_{S,T} = 0.614(kT)^2/\pi ne^4 \ln\Lambda \approx 0.06 \text{ kpc } (T/10^7 \text{ K})^2(10^{-3} \text{ cm}^{-3}/n)\,. \quad (46)$$

Functions $S_T(v)$ and $S_E(v)$ are defined by equation (36), and they are the two inhomogeneous solutions of equations (31) and (32). To find these solutions we solved equation (31) numerically by iterations. At each iteration step the integral part of this equation, $\hat{\mathcal{I}}S$, was calculated using the old solution for S from the previous step, and the new solution for S was calculated by the method of Gaussian decomposition with backsubstitution (Fedorenko 1994), using the boundary conditions of equation (32).[7] Initially, we started with zero function $S = 0$. The iterations converged very rapidly, and the Gaussian decomposition method is stable. We believe that our numerical method is much better and faster

[7] This method works as follows: At each iteration step we write the differential operator $\hat{\mathcal{L}}S$ in eq. (31) as a finite-difference operator leading to a system of linear equations for the new solution for S. This system is a tridiagonal matrix, which is solved by Gaussian decomposition with backsubstitution.

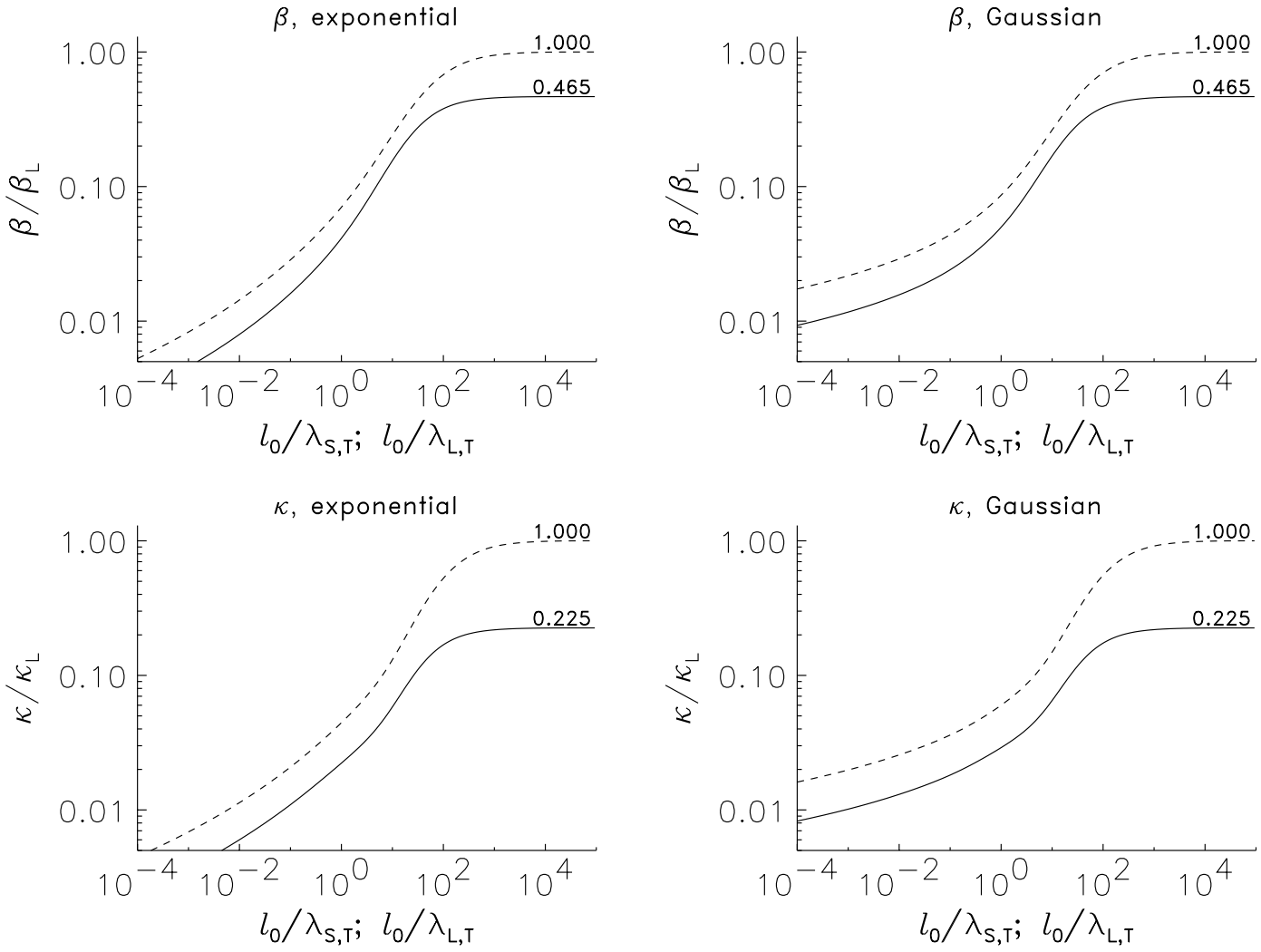

FIG. 5.—*Continued*

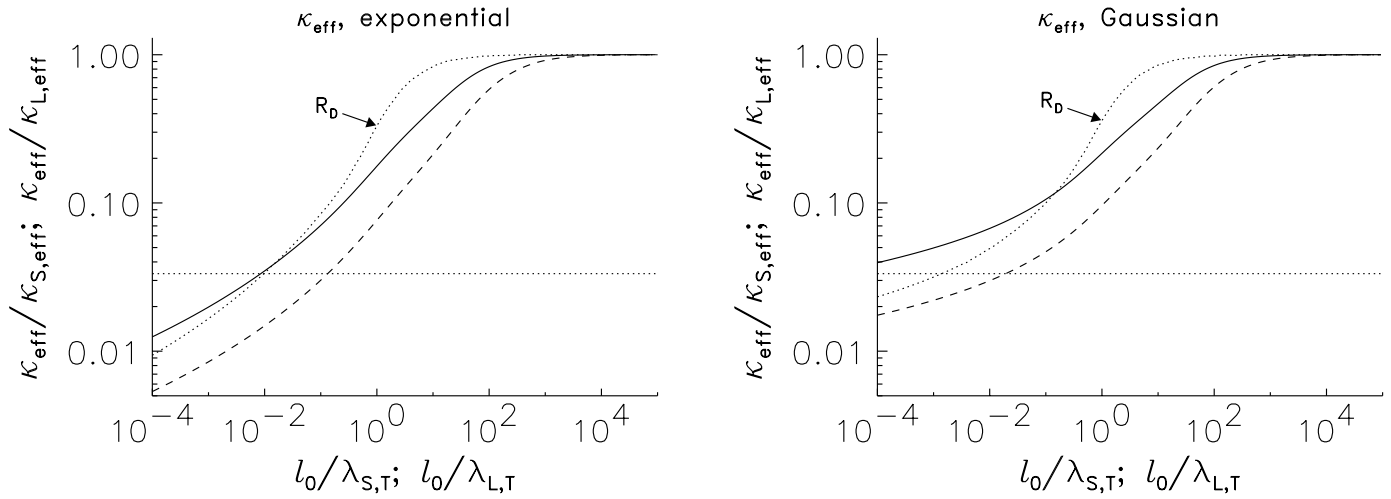

FIG. 6.—The solid/dashed lines show the reduction of the parallel effective thermal conductivity for the Spitzer/Lorentz gas by stochastic magnetic mirrors, as a function of the ratio of the magnetic field decorrelation length to the Spitzer/Lorentz electron mean free path. The notations are the same as in Fig. 5. For comparison, we give the monoenergetic diffusion reduction $R_D(l_0/\lambda_T) = D(l_0/\lambda_T)/D_0$ by the dotted lines. The horizontal dotted lines represent the reduction of 1/30; below these lines the thermal conduction is so weak that it should become negligible in clusters of galaxies.

than the method of Spitzer & Härm (1953) because their method was not stable. It took us less than 10 s of computer time to calculate all digits of the transport coefficients reported by Spitzer & Härm.

The solid lines in Figures 5*a*–5*h* show the resulting transport coefficients σ, α, β, and κ normalized to the standard Lorentz coefficients of equation (40) as functions of $l_0/\lambda_{S,T}$ for the two mirror spectra: (*a*) exponential and (*b*) Gaussian (see eq. [14]; remember that l_0 is the magnetic field decorrelation length). The asymptotic values of the coefficients at large values of $l_0/\lambda_{S,T}$ are given by the numbers on the solid lines, and they agree with the results of Spitzer & Härm.

The effective thermal conductivity, $\kappa_{\rm eff}$, normalized to the Spitzer effective conductivity, $\kappa_{S,\rm eff} = 0.0943\kappa_L$, is given in Figure 6 by the solid lines for the two mirror spectra. This normalized conductivity is the actual suppression of the effective thermal conductivity of the Spitzer gas by stochastic magnetic mirrors. *It is the result that should be applied in astrophysical problems with random magnetic mirrors.*

Finally, it is interesting to see how the mirrors change the Spitzer perturbed electron distribution function. In Figure 7 we plot functions $v^2S_T(v)$ and $v^2S_E(v)$ for the case when $l_0 = \lambda_{S,T}$ (note that $2\pi V^2 f_1$ is the actual distribution of electrons over speed $V = vV_T$; see eq. [37]). The solid lines represent these functions for the Spitzer gas in a system of random mirrors with the exponential mirror spectrum (for the Gaussian spectrum the results are similar). The dashed lines show the same functions for the Spitzer gas without magnetic mirrors. We see that $v^2S_T(v)$ and $v^2S_E(v)$ are reduced at large values of v, i.e., magnetic mirrors reduce the anisotropy of the superthermal electrons, which carry the electrical current and heat.

6. CONCLUSIONS

In this paper we have derived the actual parallel effective thermal conductivity that should be applied to astrophysical systems with random magnetic mirrors, as well as other important transport coefficients.

Now, let us apply our results for the reduction of the Spitzer effective electron thermal conductivity, shown in Figure 6 by the solid lines, to the galaxy cluster formation problem. If the reduction is by more than a factor of 30 (Fig. 6, *horizontal dotted lines*), then the time of heat transport becomes larger than the Hubble time, and the heat conduction can be neglected (Suginohara & Ostriker 1998).[8] We see that this is the case if the magnetic field decorrelation length l_0 is roughly less than 10^{-4}–10^{-2} of the electron mean free path at the thermal speed $\lambda_T = \lambda(\sqrt{2kT/m_e})$ (we consider the Spitzer gas). Although there is little observational data about the topology of magnetic fields in clusters of galaxies, the magnetic field scale is probably 1–10 kpc (Kronberg 1994; Eilek 1999 and references therein). According to equation (46) the characteristic electron mean free path at the thermal speed is 0.06–60 kpc for temperatures $T = 10^7$–10^8 K and densities $n = 10^{-4}$–10^{-3} cm^{-3}. We see that, in general, the effective electron thermal conductivity parallel to the magnetic field lines is not reduced enough by magnetic mirrors to be completely neglected. However, as we pointed out in the introductory section, there is an additional effect that electrons have to travel along tangled magnetic field lines larger distances from hot to cold regions of space, so the thermal conduction is further reduced (this effect will be considered in our future paper). At the moment, whether or not electron thermal conductivity in clusters of galaxies is sufficiently inhibited that it can be ignored is still an open question.

Recently, Cowley, Chandran, et al. studied the reduction of the parallel thermal conduction, and they concluded that the thermal conductivity in galaxy clusters is reduced enough to be neglected (Chandran & Cowley 1998; Chandran et al. 1999; Albright et al. 2000). Their conclusions are different from ours. The reason is that our approach in calculation of the conductivity is very different, and our results are qualitatively different. The main difference is that they took the reduction of thermal conductivity to be equal to the reduction of diffusivity of thermal electrons. In fact, the reduction of diffusivity is due to the enhanced pitch angle scattering by stochastic magnetic mirrors, and to find the reduction of thermal conductivity, the full set of kinetic equations must be derived and solved. This consistent way of solving the problem makes a considerable difference (see Fig. 6). On the other hand, Cowley, Chandran, et al. first

[8] See footnote 1.

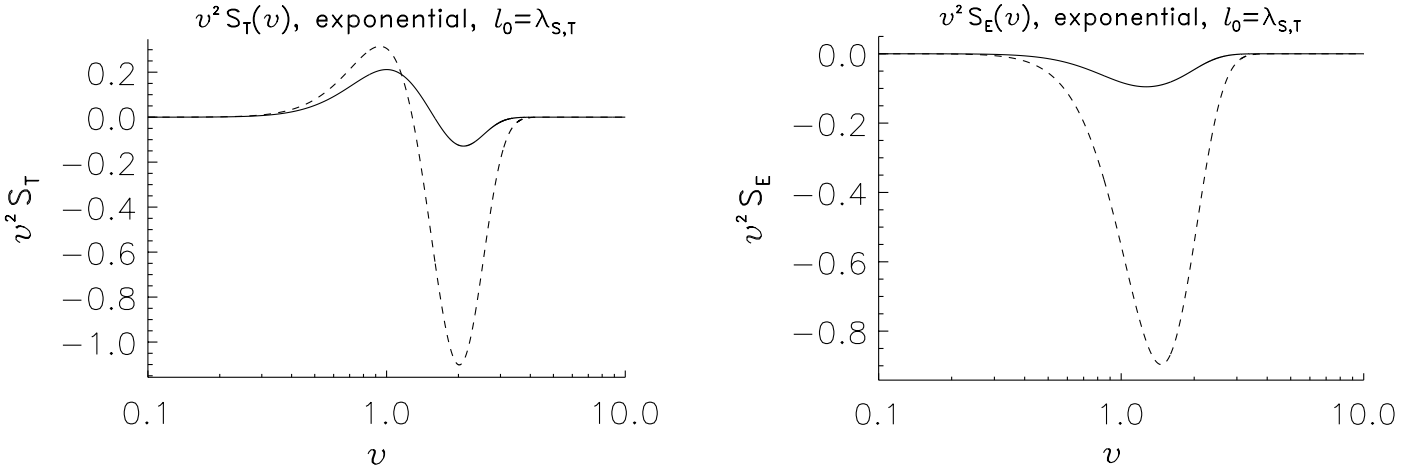

FIG. 7.—The solid lines show functions $v^2S_T(v)$ (*left panel*) and $v^2S_E(v)$ (*right panel*) for the Spitzer gas in a system of random magnetic mirrors for the case $l_0 = \lambda_{S,T}$ (l_0 is the magnetic field decorrelation length and $\lambda_{S,T}$ is the Spitzer electron mean free path; see eq. [46]). The dashed lines in the corresponding plots show the same functions for the Spitzer gas without mirrors. Both graphs are plotted for the exponential mirror spectrum (for the Gaussian spectrum the results are similar).

called attention to the importance of the effective mean free path $\lambda_{\rm eff}$ and found the correct qualitative result that in the limit $l_0 \ll \lambda$ the diffusion reduction is controlled by the mirrors whose spacing is of order of the effective mean free.

We are happy to acknowledge many useful discussions of this problem with Jeremiah Ostriker, Jeremy Goodman, and David Spergel. We would also like to thank Makoto Matsumoto, Takuji Nishimura, and Shawn J. Cokus for providing us with fast random number generators.[9] This work was partially supported by DOE under contract DE-AC 02-76-CHO-3073. Leonid Malyshkin would also like to thank the Department of Astrophysical Sciences at Princeton University for financial support.

[9] Given at http://www.math.keio.ac.jp/matumoto/emt.html.

APPENDIX A

SOLUTION OF EQUATION (3) IN THE LIMIT $l_m \ll \lambda_{\rm eff}$

Here we solve equation (3) by expansion in the limit $l_m \ll \lambda_{\rm eff}$. This condition means that collisions are too weak to scatter the electron out of the loss cones. Therefore, $F(x, \mu) \equiv 0$ when $|\mu| > \mu_{\rm crit}$.

We make use of the fact that $(V/v)(\partial/\partial x) \sim \lambda/l_m \gg 1$. Also we will show that $1/v\tau_m \ll 1$. The validity of this last assumption appears below. To zero order, we have $\partial F/\partial x = 0$ and $F(x, \mu) = F_0(\mu)$. $F_0(-\mu) = F_0(\mu)$ because of electron reflection at the mirrors and the symmetry of the loss cones. Up to first order, $F(x, \mu) = F_0(\mu) + F_1(x, \mu)$, and we have

$$\mu V \frac{\partial F_1}{\partial x} = \frac{v}{2} \frac{\partial}{\partial \mu} \left[(1 - \mu^2) \frac{\partial F_0}{\partial \mu} \right] + \frac{F_0}{\tau_m} . \tag{A1}$$

We integrate this equation over x along a closed back-and-forth trajectory of a trapped electron shown by the dotted lines in Figure 1*b* to obtain

$$\partial/\partial\mu[(1 - \mu^2)\partial F_0/\partial\mu] + 2F_0/v\tau_m = 0 , \qquad F_0(-\mu) = F_0(\mu) , \qquad F_0(\pm\mu_{\rm crit}) = 0 . \tag{A2}$$

We solve equation (A2) by a further expansion, $1/v\tau_m \ll 1$. The even solution in the "inside" region $1 - |\mu| \gg e^{-v\tau_m}$ up to first order is

$$F_0^{(i)} = C^{(i)} \left(1 - \frac{1}{v\tau_m} \ln \frac{1}{1 - \mu^2} \right) , \qquad 1 - |\mu| \gg e^{-v\tau_m} . \tag{A3}$$

On the other hand, the zero-order solution in the "boundary" regions $1 - |\mu| \ll 1$ is

$$F_0^{(b)} = C^{(b)} \ln \frac{1 - |\mu|}{1 - \mu_{\rm crit}} , \qquad 1 - \mu_{\rm crit} \leq 1 - |\mu| \ll 1 . \tag{A4}$$

We match solutions (A3) and (A4) together in regions $e^{-v\tau_m} \ll 1 - |\mu| \ll 1$ to finally obtain $\tau_m = v^{-1} \ln m$, justifying $1/v\tau_m \ll 1$. This is the first result in equation (5).

APPENDIX B

SOLUTION OF EQUATION (3) IN THE LIMITS $\lambda_{\rm eff} \ll l_m \ll \lambda^2/\lambda_{\rm eff}$ AND $\lambda^2/\lambda_{\rm eff} \ll l_m$

Let us consider the kinetic equation (3) in the more limited case $\lambda \ll l_m$ (note that $\lambda_{\rm eff} \ll \lambda$). This means that in the kinetic equation $(V/v)(\partial/\partial x) \lesssim \lambda/l_m \ll 1$. We will also show that $1/v\tau_m \ll 1$. The validity of this assumption appears below. To zero order, we have $\partial F/\partial\mu = 0$, so $F(x, \mu) = F_0(x)$. $F_0(-x) = F_0(x)$ because of symmetry. Up to first order, $F(x, \mu) = F_0(x) + F_1(x, \mu)$, and we have

$$\frac{v}{2} \frac{\partial}{\partial \mu} \left[(1 - \mu^2) \frac{\partial F_1}{\partial \mu} \right] = \mu V \frac{\partial F_0}{\partial x} - \frac{F_0}{\tau_m} . \tag{B1}$$

We integrate the above equation over μ, and then set $\mu = \pm 1$ to find the constant of integration. As a result, we obtain $F_0/\tau_m \ll V(\partial F_0/\partial x)$ (so $1/v\tau_m$ is of second order) and $\partial F_1/\partial\mu = -(V/v)(\partial F_0/\partial x)$. We integrate this last equation over μ once more and obtain

$$F_1 = -(\mu V/v)(\partial F_0/\partial x) + C(x) , \tag{B2}$$

where $C(x)$ is another integration constant.

We continue the expansion of the kinetic equation (3) to next order. Up to second order, $F(x, \mu) = F_0(x) + F_1(x, \mu) + F_2(x, \mu)$. Using equation (B2), we have

$$\frac{v}{2} \frac{\partial}{\partial \mu} \left[(1 - \mu^2) \frac{\partial F_2}{\partial \mu} \right] = -\frac{\mu^2 V^2}{v} \frac{\partial^2 F_0}{\partial^2 x} + \mu V \frac{\partial C}{\partial x} - \frac{F_0}{\tau_m} . \tag{B3}$$

We integrate equation (B3) over μ from -1 to 1 and obtain

$$\partial^2 F_0/\partial^2 x + (3\nu/\tau_m V^2)F_0 = 0 , \qquad F_0(-x) = F_0(x) . \tag{B4}$$

Finally, we integrate this equation and obtain the zero-order solution for the time-dependent distribution function (2),

$$f(t, x) = e^{-t/\tau_m} F_0(x) = e^{-t/\tau_m} \cos (x\sqrt{3\nu/\tau_m V^2}) , \tag{B5}$$

where we drop an unnecessary normalization constant of integration.

Now, to find τ_m we calculate the flux of escaping electrons through the two escape windows (see Fig. 1),

$$\partial N/\partial t = -2\int_{\mu_{\rm crit}}^{1} \mu V f(t, l_m/2)\, d\mu = -(V/m)e^{-t/\tau_m} \cos [(l_m/2)\sqrt{3\nu/\tau_m V^2}] , \tag{B6}$$

where we use equation (B5) for $f(t, l_m/2)$. On the other hand, the flux is equal to the change of the total number of electrons,

$$\partial N/\partial t = \int_{-l_m/2}^{l_m/2}\int_{-1}^{1} (\partial f/\partial t)\, d\mu\, dx = -(4/\tau_m)e^{-t/\tau_m}\sqrt{\tau_m V^2/3\nu} \sin [(l_m/2)\sqrt{3\nu/\tau_m V^2}] . \tag{B7}$$

Equating the two formulae for $\partial N/\partial t$, we obtain

$$(3/16)(\nu\tau_m/m^2) = \tan^2 \sqrt{3\nu l_m^2/4\tau_m V^2} . \tag{B8}$$

In the limit $\lambda \ll l_m \ll \lambda^2/\lambda_{\rm eff}$, the argument of the tangent above is small, so we expand the tangent and obtain $\tau_m = \nu^{-1}(l_m/\lambda_{\rm eff})$, while $F_0 \approx$ const. In the limit $\lambda^2/\lambda_{\rm eff} \ll l_m$, the left-hand side of equation (B8) is large. Therefore, the argument of the tangent is $\pi/2$, and we have $\tau_m = \nu^{-1}(3/\pi^2)(l_m/\lambda)^2$ (the third line in eq. [5]); i.e., the escape time is controlled by diffusion in x-space. In both limits $1/\nu\tau_m \ll 1$, as we assumed above, and of second order.

Now, the limit $\lambda_{\rm eff} \ll l_m \lesssim \lambda$ is still left. The result in this case is the same as the result in case $\lambda \ll l_m \ll \lambda^2/\lambda_{\rm eff}$. However, instead of solving the kinetic equation, we give the following qualitative arguments supported by our numerical simulations (see Fig. 2). The relaxation time of the electron distribution in μ-space can be estimated as $\Delta t_\mu \sim \nu^{-1}$. The relaxation time in x-space can be estimated as the crossing time $\Delta t_x \sim l_m/V = \nu^{-1}(l_m/\lambda)$ in case $l_m \lesssim \lambda$, and as the time of diffusion across $\Delta t_x \sim \nu^{-1}(l_m/\lambda)^2$ in case $\lambda \ll l_m$. All relaxation times are small compared to the escape time τ_m, i.e., Δt_μ, $\Delta t_x \ll \tau_m$ for the entire range $\lambda_{\rm eff} \ll l_m \ll \lambda^2/\lambda_{\rm eff}$. This means that the distribution function is approximately constant in x and μ, say $F_0 \approx 1$, $f \approx e^{-t/\tau_m}$. We then carry out calculations similar to those we used in formulae (B6) and (B7) to find that $\tau_m = \nu^{-1}(l_m/\lambda_{\rm eff})$ (the second line in eq. [5]).

APPENDIX C

THE ADDITIONAL ELECTRON FLOW PRODUCED BY ELECTRIC FIELD

Let us, for simplicity, consider the Lorentz gas. The results for the Spitzer gas are similar.

First, we derive an estimate for the additional flow $d\tilde{\mathcal{F}}$ of electrons that are in an interval $V \in [V, V + dV)$ of the velocity space, produced by an electric field E due to the change of the two loss cones of a mirror trap. Let us consider only the principal mirrors, because they mainly control the diffusion of electrons (see § 3). In this appendix, we denote their mirror strength (the principal mirror strength) as M.

The principal mirror strength is of order of 5, so in the case when the magnetic field decorrelation length is more than or approximately equal to the electron mean free path, $l_0 \gtrsim \lambda$, the escape of electrons from the mirror trap is mainly controlled by their spatial diffusion (see § 2). Thus, in this limit, the electrons "do not care" about the size of the loss cones, and therefore, no additional flow arises.

In the case $l_0 \lesssim \lambda$, there is a nonzero additional flow $d\tilde{\mathcal{F}}$. In Figure 1*b*, because of the electric field, the loss cone on the left, $\mu_{{\rm crit},-}$, is not equal to that on the right, $\mu_{{\rm crit},+}$. The size of the two loss cones is estimated from the conservation of the electron magnetic moment, $(1 - \mu^2)V^2/B =$ const, and from the conservation of energy, $m_e V^2/2 + eEx =$ const. We have

$$\mu_{{\rm crit},\pm}^2 \approx 1 - 1/M \pm (eEl_M/m_e V^2 M) , \tag{C1}$$

where l_M is the spacing of the principal mirrors.

Let $d\tilde{\mathcal{F}}_+$ and $d\tilde{\mathcal{F}}_-$ be the absolute values of the fluxes of the escaping electrons to the right and to the left, respectively. Then, their sum is

$$d\tilde{\mathcal{F}}_+ + d\tilde{\mathcal{F}}_- = (l_M/\tau_M)2\pi V^2 f_0\, dV , \tag{C2}$$

where $2\pi V^2 f_0\, dV$ is the number density of electrons expressed in terms of the Maxwellian zero-order electron distribution function f_0, and τ_M is the escape time (see eqs. [2], [6], and [16] and § 2). The actual electron flow, $d\tilde{\mathcal{F}}$, is equal to the difference of $d\tilde{\mathcal{F}}_+$ and $d\tilde{\mathcal{F}}_-$, because they are in opposite directions. An estimate for the ratio $d\tilde{\mathcal{F}}/(d\tilde{\mathcal{F}}_+ + d\tilde{\mathcal{F}}_-)$ is

$$\frac{d\tilde{\mathcal{F}}}{d\tilde{\mathcal{F}}_+ + d\tilde{\mathcal{F}}_-} = \frac{d\tilde{\mathcal{F}}_+ - d\tilde{\mathcal{F}}_-}{d\tilde{\mathcal{F}}_+ + d\tilde{\mathcal{F}}_-} \approx \left(\int_{\mu_{{\rm crit},+}}^{1} \mu\, d\mu - \int_{\mu_{{\rm crit},-}}^{1} \mu\, d\mu\right)\left(\int_{\mu_{{\rm crit},+}}^{1} \mu\, d\mu + \int_{\mu_{{\rm crit},-}}^{1} \mu\, d\mu\right)^{-1} . \tag{C3}$$

Now, using equations (C1)–(C3), we obtain the additional electron flow

$$d\tilde{\mathcal{F}} \approx -2\pi(eE/m_e) f_0 (l_M^2/\tau_M)\, dV . \tag{C4}$$

The factor (l_M^2/τ_M) in this equation is proportional to the spatial diffusivity of the electrons (provided that the diffusivity is controlled by the principal mirrors; see § 3). Thus, it is obviously $l_M^2/\tau_M = R_D \lambda_L^2 \nu_L$, where λ_L and ν_L are the standard Lorentz mean free path and collision frequency, and R_D is the reduction of the spatial diffusivity reported in § 3. Using $\lambda_L \propto V^4$, $\nu_L \propto V^{-3}$, and equations (16), (43), and $V_T = (2kT/m_e)^{1/2}$, we finally obtain

$$d\tilde{\mathcal{F}} \approx -(1/2)(2/\pi)^{3/2}(k^{3/2}T^{3/2}E/m_e^{1/2}\, e^3 \ln\Lambda) R_D\, \upsilon^5 e^{-\upsilon^2}\, d\upsilon\ . \tag{C5}$$

Now we would like to compare this result for the additional flow $d\tilde{\mathcal{F}}$ with the main flow $d\mathcal{F}$ produced by the electric field due to acceleration of particles. The latter is

$$d\mathcal{F} = \int_{-1}^{1} \mu V f_1\, d\mu 2\pi V^2\, dV\, d\mu = -(2/3)(2/\pi)^{3/2}(k^{3/2}T^{3/2}E/m_e^{1/2}\, e^3 \ln\Lambda) R_D\, \upsilon^7 e^{-\upsilon^2}\, d\upsilon\ , \tag{C6}$$

where we substituted function f_1 given by equation (17) and function $S(\upsilon) = \gamma_E S_E(\upsilon)$ given by equations (33) and (39). As a result,

$$d\tilde{\mathcal{F}}/d\mathcal{F} \approx (3/4)\upsilon^{-2}\ . \tag{C7}$$

Because the electrical current and the heat flow are mainly transported by superthermal electrons $\upsilon^2 \sim 4$, the additional flow produced by electric field due to nonequal loss cones can indeed be neglected in comparison with the main flow due to acceleration of electrons by electric field.

REFERENCES

Albright, B. J., Chandran, B. D. G., Cowley, S. C., & Loh, M. 2000, Phys. Plasmas, in press (PoP-24828)
Braginskii, S. I. 1965, Rev. Plasma Phys., 1, 205
Cen, R., & Ostriker, J. 1999, ApJ, 514, 1
Chandran, B. D. G., & Cowley, S. C. 1998, Phys. Rev. Lett., 80, 3077
Chandran, B. D. G., Cowley, S. C., & Ivanushkina, M. 1999, ApJ, 525, 638
Cohen, R. S., Spitzer, L., Jr., & Routly, P. M. 1950, Phys. Rev., 80(, 230
Eilek, J. 1999, Proc. Workshop Diffuse Thermal and Relativistic Plasma in Galaxy Clusters, ed. H. Böhringer, L. Feretti, P. Schuecker, & V. K. Kapahi (MPE Rep. 271; Garching: Max-Planck-Institut fur extra-terrestrische Physik), 71
Fabian, A. C. 1990, Physical Processes in Hot Cosmic Plasmas, ed. W. Brinkmann, A. C. Fabian, & F. Giovanelli (NATO ASI Ser. C, 305; Dordrecht: Kluwer), 210
Fedorenko, R. P. 1994, Introduction to Computational Physics (Moscow: Moscow Inst. Physics & Tech. Press)
Kronberg, P. P. 1994, Rep. Prog. Phys., 57, 325
Pistinner, S., & Shaviv, G. 1996, ApJ, 459, 147
Rosenbluth, M. N., MacDonald, W. M., & Judd, D. L. 1957, Phys. Rev., 107, 1
Rosner, R., & Tucker, W. H. 1989, ApJ, 338, 761
Spitzer, L., Jr. 1962, Physics of Fully Ionized Gases (New York: Wiley)
Spitzer, L., Jr., & Härm, R. 1953, Phys. Rev., 89, 977
Suginohara, T., & Ostriker, J. 1998, ApJ, 507, 16
Tao, L. 1995, MNRAS, 275, 965
Tribble, P. C. 1989, MNRAS, 238, 1247